BioEnergy Research (2019) 12:1052–1065
https://doi.org/10.1007/s12155-019-10027-4

Influence of Process Parameters on Optimization of Biochar Fuel Characteristics Derived from Rice Husk: a Promising Alternative Solid Fuel

Krishna Yadav[1] · Megha Tyagi[1] · Soni Kumari[1] · Sheeja Jagadevan[1]

Published online: 23 August 2019

Abstract

Process parameters play a crucial role in governing the physical and chemical properties of biochar. An optimization tool, response surface methodology (central composite design) was employed to identify the linear and interaction effects of process parameters (temperature, heating rate and time) on selected responses, namely biochar yield, higher heating value, energy density and energy yield of biochar. The optimized values for temperature, heating rate and time were found to be 432 °C, 4 °C/min and 40 min respectively. At these optimized conditions, the biochar yield, higher heating value, energy density and energy yield of biochar were found to be 54.65%, 25.08 MJ/kg, 1.46 and 79.66% respectively. The fuel ratio of optimized biochar was found to be 2.10 which is near to that of bituminous coal having fuel ratio in range of 1.5 to 2.0. This study performs an in-depth qualitative and quantitative analysis of the synthesized biochar so as to ensure higher yield and improved quality of solid fuel for possible practical utility. The thermal conversion of biomass can therefore be a potential route to provide an economically viable, clean and environment friendly source of good quality solid fuel through utilization of biomass or biomass-derived waste.

Keywords Biochar · Fuel ratio · Pyrolysis · Response surface methodology · Rice husk · Solid fuel

Introduction

Asia is one of the largest producers of paddy and generates approximately 45 million tonnes of rick husk [1]. As a by-product of rice production, this rice husk is majorly of no commercial value [1]. The residual rice husk is conventionally either burnt in the agricultural field or dumped as waste, causing environmental pollution. We aim to exploit this waste product to useful product, i.e. biochar with huge applicability in form of solid fuel. Rice husk biomass, which is typically composed of cellulose, hemicelluloses and lignin, offers great potential to be employed as an alternate source of energy via thermochemical conversion processes [2]. Amongst the available conversion techniques, namely liquefaction, torrefaction, pyrolysis and gasification, pyrolysis is considered to be the most efficient technique used for conversion of biomass into a value-added biochar (solid fuel), liquid and gaseous products through heating in an oxygen limited environment [3, 4]. In addition, pyrolysis brings forth degradation of biomass into mixture of organic and inorganic compounds. The reaction mechanism for pyrolysis process can be summarized in three successive steps as given below [5].

(Step 1) Raw biomass → moisture + unreactive residues
(Step 2) Unreactive residues → volatiles + gas + primary biochar
(Step 3) Primary biochar → volatiles + gas + secondary biochar

In the initial step, moisture is primarily lost from the raw biomass and the second step leads to the synthesis of primary biochar. The final and rate-determining step involves decomposition of primary biochar at very slow rate, resulting in the production of carbon-rich solid residue, i.e. secondary biochar along with volatiles and gaseous products. The obtained biochar is carbonaceous, fine-grained and a porous substance having low moisture content and higher heating value.

Electronic supplementary material The online version of this article (https://doi.org/10.1007/s12155-019-10027-4) contains supplementary material, which is available to authorized users.

✉ Sheeja Jagadevan
sheejaj@iitism.ac.in

[1] Department of Environmental Science and Engineering, Indian Institute of Technology (Indian School of Mines), Dhanbad, Jharkhand 826004, India

Biochar has multiple applications in various fields as it leads to climate stability, soil health and in water and wastewater treatment [6, 7], owing to its typical properties such as high surface area, high adsorption capacity and high cation exchange capacity [7–9]. Although, biochar has a unique ability to bind with organic and inorganic contaminants through charged functional groups, making them capable to adsorb contaminants generated from soil, water and wastewater [8]. Biochar fuel has several advantages such as high-energy density, higher boiler efficiency concomitant with lower corrosion effect on surface of boilers owing to its lesser sulphur content, low moisture content, lower ash content as compared to fossil coal, more uniform combustion, carbon credit benefits, ease in handling and transportation [9]. The low cost and ease of availability further make rice husk a suitable feedstock for biochar production, serving as an alternative source of solid fuel.

The quality of biochar depends on the physicochemical properties (moisture content, volatile content, fixed solid carbon content, pH, higher heating value and percentage of carbon). The physical and chemical properties of solid fuel is closely dependant on the organic constituents of biomass (cellulose, hemicellulose and lignin) and process parameters such as temperature, time, heating rate, purging gas, particle size and pressure employed for pyrolysis [2, 3, 9–11]. Pyrolytic temperature is negatively correlated with the biochar yield, as enhancement in temperature leads to thermal cracking of high molecular weight hydrocarbons present in the biomass. This increases the production of liquid and gaseous products, but the biochar yield decreases [3]. Longer residence time provides a greater chance for re-polymerization of the constituents of biomass, thereby enhancing the biochar yield. The rate of change of heat during pyrolysis plays a key role in the distribution of solid, liquid and gaseous products. Moreover, biochar produced at greater pyrolysis temperature results in biochar fuel having higher heating value and energy density. Energy yield is invariably dependent on biochar yield and higher heating value. Energy yield is negatively correlated with process parameters such as temperature, time and heating rate due to the occurrence of thermal cracking at elevated pyrolysis conditions [12]. Therefore, the quantity and quality of a solid fuel could be assessed by its yield, higher heating value, energy density, energy yield and fuel ratio.

Literature survey reveals very few studies which have reported biochar produced from waste biomass as a source of fuel, and these studies have scarcely reported the detailed characteristics of biochar fuel [13–17]. In these studies, the individual process parameters have been studied in detail, but the interaction between biochar preparation conditions and biochar fuel characteristics have not been much explored. The present study focusses on the interaction effects of key process parameters such as pyrolysis temperature, time and heating rate on biochar yield, higher heating value, energy density and energy yield of biochar fuel using response surface methodology (RSM). RSM is a statistical and mathematical tool which provides an effective way to optimize process parameters in order to get optimal output with least number of experiments.

This study focuses on the effect of the pyrolysis temperature, time and heating rate on the quality (heating value, energy density) and yield of the synthesized biochar, which has been rarely studied. The proximate and ultimate analysis, atomic ratio, pH and calorific value of the optimized biochar are also reported. Furthermore, spectral, morphological and thermogravimetric analyses have been carried out to assess the changes occurring during the pre- and post pyrolysis steps.

Materials and Methods

Synthesis of Biochar

Rice husk was collected from a rice mill located at Salempur village of Mau district, Uttar Pradesh (26° 03′ 30.7″ N, 83° 26′ 42.3″ E). The biomass was washed thoroughly with deionised water (type-I water) and crushed into small pieces (~ 10 mm) using a mixer grinder. These were then oven-dried for 24 h at 105 ± 5 °C and pyrolyzed (under oxygen limited condition) in a tube furnace (Antslab™, India). The biochar was then ground using mortar-pestle and sieved using 210–105 μm sieve.

Characterization of Biochar

Proximate Analysis

The proximate analysis included moisture content, volatile matter, ash content and fixed carbon. The moisture content was calculated by drying the biomass and biochar samples at 105 °C, as per ASTM D2867-09. The volatile matter and ash content were determined by following ASTM D5832-98 and ASTM D2866-11 methods respectively. The fixed solid carbon content was calculated from these values, as given in Eq. (1).

$$\text{Fixed solid carbon content }(\%) = [100-(\text{volatile content} + \text{ash content} + \text{moisture content})] \quad (1)$$

The chemical composition of cellulose (%), hemicellulose (%), lignin (%) and extractives (%) in the raw biomass was determined by the method prescribed by Lin et al. [18].

Ultimate Analysis

The percentage elemental composition of carbon, hydrogen and nitrogen was determined by elemental analyzer

(EA3000, EuroVector, Italy). The percentage of oxygen was then calculated by using the expression given in Eq. (2).

$$\text{Oxygen }(\%) = [100-(\text{C}+\text{H}+\text{N})] \quad (2)$$

The ratios of O/C, H/C and (O+N)/C were calculated to determine the hydrophilicity index, aromaticity index and polarity index respectively [19].

The pH of biochar produced at different process parameters was determined by the addition of biochar to deionised water in mass ratio of 1:10, and the resulting suspension was mixed for 1 h [20]. The pH was then measured with a pH meter (OAKTON pH 700). Fuel ratio (FR) was calculated using the expression given in Eq. (3).

$$\text{FR} = [\text{Fixed solid carbon content }(\%)/\text{Volatile matter }(\%)] \quad (3)$$

Spectral, Morphological and Thermogravimetric Analyses

Spectral behaviour of rice husk and biochar was measured with the help of Fourier transform infrared spectroscopy (FTIR) (PerkinElmer 2000, USA). The spectra were recorded in the range of 400 to 4000 cm^{-1} [21]. The morphology of raw biomass and optimized biochar was determined using field emission scanning electron microscope (Carl Zeiss-SUPRA 55, Germany). Rice husk–derived biochar was characterized using various techniques to determine the elemental composition and morphology [22]. Thermogravimetric (TG) analysis of rice husk and biochar was carried out with the help of a TG analyser (Mettler Toledo thermogravimetric analysis (TGA)/DSC instrument coupled with differential scanning calorimetry) under nitrogen atmosphere (flow rate 25 mL/min), heated from temperature 30 to 800 °C (heating rate 10 °C/min) [23].

Experimental Design

Design of experiment and optimization of process parameters were done with the help of response surface methodology (RSM) using Design Expert software (version 7.0.0, Stat-Ease Inc., Minneapolis, USA) [24]. RSM is a mathematical and statistical tool which provides an effective way to optimize process parameters with minimum number of experiments [25, 26]. Central composite design (CCD), a popular design used in response surface methodology (RSM), was employed to evaluate the optimum conditions for biochar synthesis. A three-factor, five-level CCD consisting of 20 experimental runs (8 factorial, 6 axial and 6 central point) were performed. Total number of experiment was calculated by $N = 2^n + 2n + C_n$, where N is total number of runs and n is number of independent variables. The term 2^n represents the number of factorials runs, $2n$ is axial runs and C_n is central runs [27]. The experimental error and reproducibility of the data could be gathered from the centre points. Three independent variables, i.e. temperature, retention time and heating rate, were chosen in this study.

Four responses were therefore selected in this design: (i) Yield of biochar (%) [(Weight of biomass − Weight of biochar)/Weight of biomass × 100]. Several previous studies have indicated that higher biochar yield makes the thermal process more viable and economical [9, 28]. (ii) Higher heating value (HHV) (MJ/kg) $[(0.605 \times \%\text{C}) + (1.352 \times \%\text{H}) + (0.84 \times \%\text{N}) + (0.275 \times \%\text{ash}) - 26.29]$ as given in Mesroghli et al. [29]; (iii) Energy density (ED) [(Biochar HHV/Biomass HHV)]; (iv) Energy yield (EY) (%) [(Biochar yield × Energy density)]. The higher heating value, energy density and energy yield of biochar are interrelated and define the quality of the solid fuel [9, 28, 30]. In order to get an improved quality of solid fuel, HHV, ED and EY should be high. Table 1 shows the experimental ranges of the independent variables employed in the present study, which were fixed on the basis of preliminary trial experiments. The responses obtained from all experimental runs were then adjusted by first-, second- and third-order polynomial equations. The effects of the main variables and their interaction effects were estimated by analysis of variance (ANOVA). Fitness of the model and significant terms in the model were evaluated by the correlation coefficient (R^2), probability (p value), lack of fit and Fisher's (F test). The interaction amongst variables was analyzed using three-dimensional response surface plots.

Results and Discussion

Proximate Analysis of Biomass and Optimized Biochar

The proximate analysis of biomass and biochar produced at different experimental conditions (20 runs) is given in Table 2. The percentage of moisture content and volatile matter in untreated biomass was found to be 9.02 and 70.64 respectively, whereas for the optimized biochar (OBC), these values reduced considerably to 2.94% and 17.88%. The decrease in moisture content and volatile matter is due to the dehydration of hydroxyl groups and thermal degradation of cellulose and

Table 1 Experimental parameters and their ranges employed in central composite design

Parameters	Symbols	Levels				
		$-\alpha$	-1	0	$+1$	$+\alpha$
Temperature (°C)	*A*	298.87	350	425	500	551.13
Time (min)	*B*	34.89	40	47.5	55	60.11
Heating rate (°C/min)	*C*	2.98	4	5.5	7	8.02

Table 2 Proximate analysis of biomass and biochar produced at different experimental condition

Run	Process parameters			Proximate analysis				pH	Fuel ratio
	Temperature (°C)	Time (min)	Heating rate (°C/min)	Moisture content (%)	Volatile matter (%)	Ash content (%)	Fixed solid carbon content (%)		
1	500	40	4	2.14	10.27	56.14	31.45	6.2	3.06
2	425	47.5	5.5	3.27	40.37	44.35	12.01	6	0.30
3	350	40	4	4.93	54.78	28.91	11.38	4.92	0.21
4	500	40	7	2.34	10.17	56.54	30.95	5.92	3.04
5	350	55	4	5.03	53.98	32.16	8.82	5.0	0.16
6	425	47.5	2.98	2.69	40.03	42.35	14.92	5.79	0.37
7	425	47.5	5.5	2.99	40.13	45.79	11.10	6.16	0.28
8	425	47.5	5.5	3.15	39.84	44.45	12.56	6.1	0.32
9	425	47.5	8.02	3.48	39.43	44.85	12.24	5.81	0.31
10	425	34.89	5.5	3.22	41.03	43.79	11.97	5.49	0.29
11	350	55	7	4.97	52.42	34.73	7.88	5.71	0.15
12	425	47.5	5.5	3.28	40.17	44.8	11.75	6.25	0.29
13	551.13	47.5	5.5	2.04	8.56	58.27	31.13	6.7	3.64
14	298.87	47.5	5.5	6.92	62.8	25.58	4.70	4.9	0.07
15	425	47.5	5.5	3.13	40.16	45.7	11.01	6.05	0.27
16	350	40	7	5.18	53.37	31.73	9.73	4.74	0.18
17	425	47.5	5.5	3.10	40.38	45.82	10.70	6.31	0.26
18	425	60.11	5.5	3.53	38.69	46.03	11.75	6.17	0.30
19	500	55	4	2.03	9.85	57.79	30.33	5.77	3.08
20	500	55	7	2.01	9.83	59.62	28.53	5.91	2.90
Biomass	–	–	–	9.02	70.64	17.98	2.36	4.6	0.03
OBC	432	40	4	2.94	17.88	41.62	37.56	5.1	2.10

HHV high heating value, *OBC* optimized biochar

lignin constituents occurring at higher temperatures [31]. The ash content and fixed solid carbon content increased from 17.98% and 2.36% in biomass to 41.62% and 37.56% in the optimized biochar. The presence of organic matter along with inorganic minerals increased ash content on increasing the pyrolysis temperature [32]. The synchronous increase in fixed solid carbon content at higher pyrolytic temperature indicates that the carbon present in biochar was more stable than carbon found in biomass [33].

Raw biomass, which was pyrolyzed at higher temperature and for longer residence time with high heating rate, exhibited high pH. This may be due to the likely separation of alkali salts from organic matrix occurring at high temperature. In contrast, dissociation of biomass materials such as cellulose and hemicelluloses leading to the formation of organic acids and phenolic products may be responsible for lowering the pH at lower temperatures [31]. When biomass was subjected to high heating rate for longer time intervals, pH of the biochar initially showed an increasing trend, but after some time, the pH started decreasing, as shown in Table 2. The decline in pH could be attributed to depolymerization of the product formed during the course of the reaction [34, 35].

The fuel ratio invariably depends on fixed solid carbon and volatile matter content and so increases at elevated pyrolysis conditions due to thermal degradation of cellulosic, hemi-cellulosic and lignin content. The fuel ratio for rice husk and optimized biochar was found to be 0.03 and 2.10 respectively. The fuel ratio of the optimized biochar is very similar to that of bituminous coal which is typically in the range of 1.5 to 2.0 [36]. The rice husk–based biochar synthesized in this study therefore holds great potential to be used as an alternative solid fuel. Additionally, compositional analysis for rice husk biomass was carried out and cellulose, hemicellulose, lignin and extractives were found to be 49.82%, 15%, 30% and 5.18% respectively.

Ultimate Analysis of Biomass and Optimized Biochar

Table 3 presents the ultimate analysis of raw biomass and the optimized biochar, wherein percentage of carbon content is shown to increase from 38.63% in rice husk to 56.29% in OBC. Synchronous with this increment in the carbon content (~45.72%), the corresponding percentage of H, N and O in the biochar decreased considerably

Table 3 Ultimate analysis of biomass and biochar

Run	Process parameters			Ultimate analysis				Atomic ratio		
	Temperature (°C)	Time (min)	Heating rate (°C/min)	%C	%H	%N	%O	O/C	H/C	(O + N)/C
1	500	40	4	56.63	3.96	0.39	39.02	0.69	0.07	0.70
2	425	47.5	5.5	52.61	4.45	0.44	42.50	0.81	0.08	0.82
3	350	40	4	50.72	6.32	0.60	42.37	0.84	0.12	0.85
4	500	40	7	58.65	3.31	0.27	37.77	0.64	0.06	0.65
5	350	55	4	50.30	5.63	0.34	43.74	0.87	0.11	0.88
6	425	47.5	2.98	52.30	5.82	0.23	41.65	0.80	0.11	0.80
7	425	47.5	5.5	51.98	4.36	0.48	43.18	0.83	0.08	0.84
8	425	47.5	5.5	52.41	4.40	0.40	42.80	0.82	0.08	0.82
9	425	47.5	8.02	53.80	4.13	0.39	41.68	0.77	0.08	0.78
10	425	34.89	5.5	51.60	4.36	0.28	43.75	0.85	0.08	0.85
11	350	55	7	51.43	5.26	0.60	42.72	0.83	0.10	0.84
12	425	47.5	5.5	52.09	4.42	0.47	43.02	0.83	0.08	0.83
13	551.13	47.5	5.5	60.77	2.04	0.26	36.93	0.61	0.03	0.61
14	298.87	47.5	5.5	48.82	8.68	1.01	41.49	0.85	0.18	0.87
15	425	47.5	5.5	52.31	4.46	0.48	42.75	0.82	0.09	0.83
16	350	40	7	50.82	4.51	0.37	44.30	0.87	0.09	0.88
17	425	47.5	5.5	52.22	4.43	0.48	42.88	0.82	0.08	0.83
18	425	60.11	5.5	53.95	3.31	0.43	42.32	0.78	0.06	0.79
19	500	55	4	57.45	3.31	0.36	38.89	0.68	0.06	0.68
20	500	55	7	58.26	3.33	0.60	37.81	0.65	0.06	0.67
Biomass	–	–	–	38.63	10.27	1.45	49.65	1.29	0.27	1.32
OBC	432	40	4	56.29	3.71	0.52	39.48	0.70	0.07	0.71

O/C hydrophilicity index or biochar stability, *H/C* aromaticity index, *(O + N)/C* polarity index, *OBC* optimized biochar

(Table 3). This decline may be attributed to the breakdown of weak bonds associated with polymeric structure of lignocelluloses at higher temperatures. However, time and heating rate did not have much effect on percentage of carbon, hydrogen, nitrogen and oxygen.

Atomic ratios of oxygen and carbon (O/C) and hydrogen and carbon (H/C) can be used as an indicator of degree of carbonization, stability and aromaticity of biomass-derived biochar [37]. For the optimized biochar, the O/C ratio and H/C ratio were found to be 0.70 and 0.07 respectively, as against 1.29 and 0.27 for the raw biomass, thereby suggesting that the temperature applied was sufficient for successful conversion of biomass into biochar (Table 3). In general, the atomic ratios of O/C and H/C were found to be higher at lower temperature and vice versa, thus indicating that the produced biochar was highly carbonized and exhibited high aromaticity. Furthermore, the surface of biochar was less hydrophilic due to the removal of oxygen at higher temperatures [38]. Li et al. [39] reported that biochar produced at elevated temperature was basic in nature due to loss of oxygen. Van-Krevelen plot also suggested that lower atomic ratios of H/C and O/C were necessary for the successful conversion of lignocellulosic part of biomass into more hydrophobic and stable biochar [40] (Fig. 1).

Temperature emerged as the most critical factor for determining the polarity index of rice husk–derived biochar. The polarity index (O + N)/C of OBC decreased from the initial biomass, suggesting that the produced biochar was highly aromatic and less polar in nature. This is the result of the high degree of carbonization of organic matter present in the raw biomass and also due to the removal of polar surface functional groups [38]. Furthermore, on increasing the heating rate, the polarity index slightly increased initially and then a decline in the index was observed. Such a trend could be due to the high degree of carbonization and dominance of secondary pyrolysis, which leads to the formation of various gaseous components at high heating rate [11].

Spectral, Morphological and Thermogravimetric Analyses

FTIR analysis was performed to identify the functional groups present on the surface of biomass and optimized biochar. The FTIR spectra are broadly divided into three distinct bands in

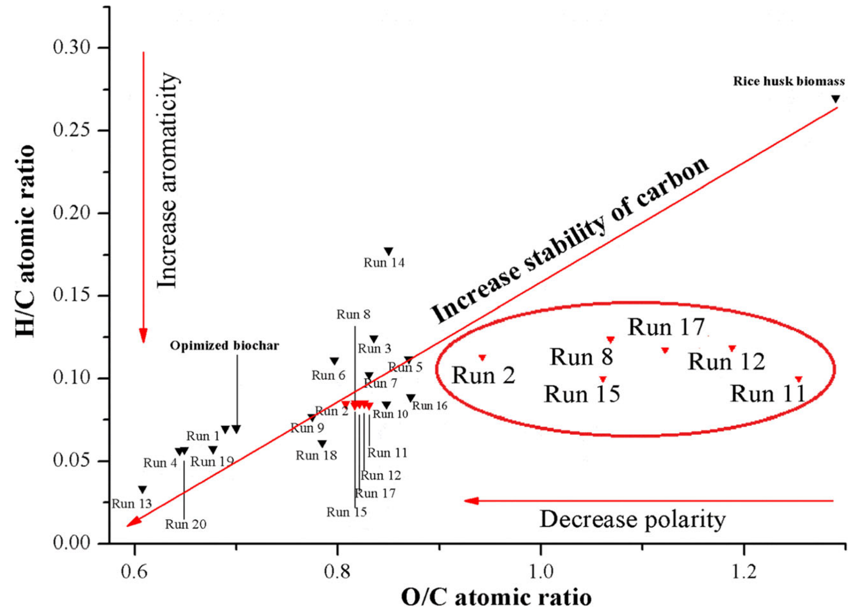

Fig. 1 Van Krevelen plot for biomass and biochar produced at different process parameters

the wavenumber range of 3424–2916 cm^{-1}, 1700–1096 cm^{-1} and 798–463 cm^{-1} (Fig. S1). The degradation of cellulose and hemicelluloses in the biomass constituents brought forth decrease in the O-H stretching region, suggesting degradation of phenolic compound present in the biomass [41]. At elevated temperatures, loss of aliphatic C-H (2961 cm^{-1}), carbonyl (1700 cm^{-1}) and hydroxyl groups (3426 cm^{-1}) were observed, indicating the occurrence of decarboxylation, decarbonylation and dehydration reactions [21]. Such reactions lead to the formation of carbonized aromatic compounds containing C=C bond and oxygen functional groups [42].

The structural and morphological changes in biomass and optimized biochar are presented in the micrographs of the field emission scanning electron microscope. The surface morphology of biomass exhibited smooth and globular structure (Fig. 2a), whereas the biochar showed irregular cells with rough surfaces (Fig. 2b) [43]. Pyrolysis parameters affect the size and shape of particles by increasing the proportion of voids [22]. The rough and porous nature of biochar is due to the evaporation of volatile materials from the biomass [44].

Thermogravimetric analysis (TGA) gives an insight about the thermal degradation of the lignocellulosic component of rice husk biomass (Fig. S2). The TGA plot of the raw biomass (Fig. S2a) shows weight loss of 5.18% and 58.71%, which could be attributed to the loss of moisture content and volatile matter respectively. The remaining is contributed by the residual matter, i.e. biochar (Fig. S2a) [23, 32]. For the biochar, such gradations were not prominent (Fig. S2b). The inverted peak of the derivative thermogravimetric (DTG) plot corresponds to the rate of weight loss of biomass and biochar. The TGA and DTG plots of biochar shifted towards higher range of temperature, thereby indicating a higher stability of biochar [40]. The DTG plot for rice husk was narrower when compared to that of biochar. For rice husk, the rate of decomposition of cellulose occurred rapidly at 371 °C, when compared to the decomposition of hemicellulose (319 °C). In contrast, for biochar, the rate of decomposition was found to be much slower and cellulose and hemicellulose decomposition were found to occur at 461 °C and 340 °C respectively. Lignin, being primarily composed of benzene rings, is very difficult to decompose. Based on the result of TGA and DTG plots, maximum degradation of biomass was inferred to be occurring between temperature range of 300–469 °C and no appreciable degradation of biomass was observed above 469 °C.

Effect of Process Variables on Biochar Yield, Higher Heating Value, Energy Density and Energy Yield

To examine the effects of pyrolysis temperature (A), pyrolysis time (B) and heating rate (C) on yield, higher heating value (HHV), energy density (ED) and energy yield (EY) of biochar, 20 experiments were run. Table 4 shows the experimental design matrix and their corresponding responses. Experimental values showed that the biochar yield, HHV, ED and EY varied between 35.38 to 60.38%, 19.59 to 30.36 MJ/kg, 1.14 to 1.77 and 60.89 to 80.61% respectively. Model equations which show empirical relationship between the three factors and

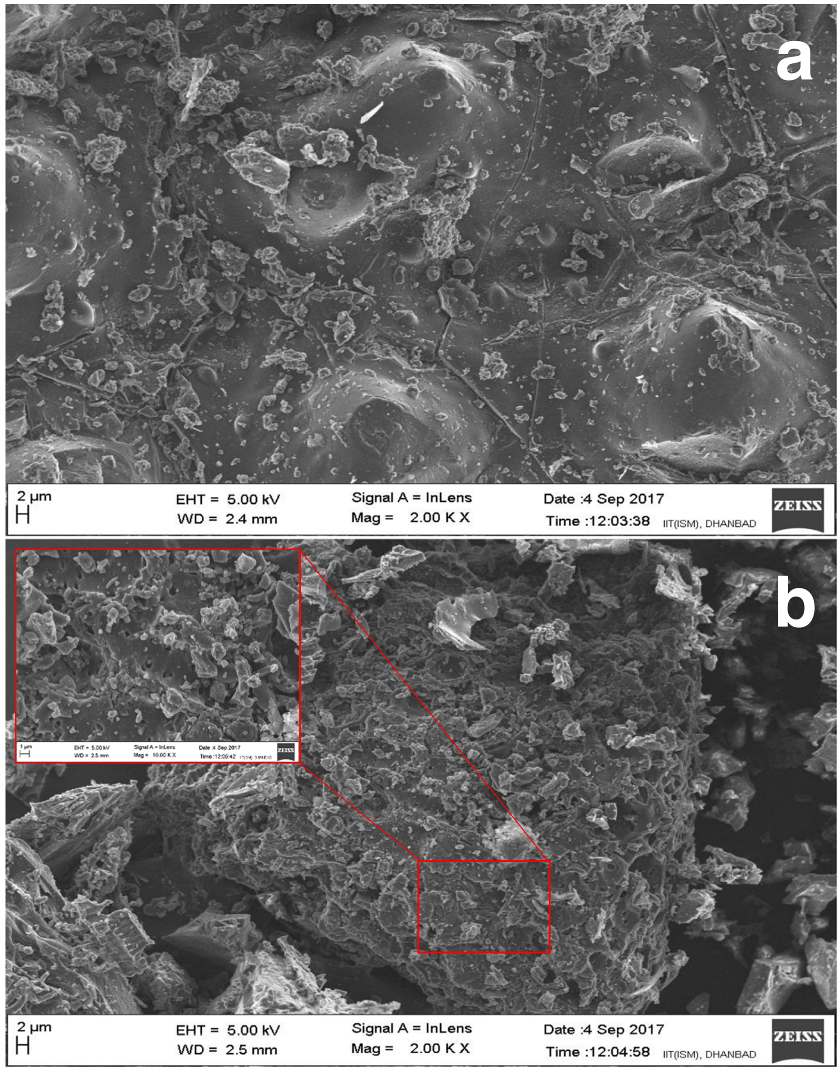

Fig. 2 FE-SEM micrograph of **a** rice husk before pyrolysis and **b** optimized biochar

responses (yield of biochar, HHV, ED and EY of biochar) were generated and could be expressed by the following model equations:

$$\begin{aligned}\text{Yield}\ (\%) = {} & 51.54 - 7.30A - 1.29B - 1.29C - 1.03AB \\ & + 0.59AC + 0.79BC - 1.53A^2 + 0.40B^2 \\ & + 0.052C^2\end{aligned} \tag{4}$$

$$\begin{aligned}\text{HHV}(MJ/kg) = {} & 24.10 + 1.97A + 0.22B - 0.17C \\ & - 0.11AB + 0.29AC + 0.47BC \\ & + 0.81A^2 - 0.14B^2 + 0.32C^2 \\ & - 0.25ABC + 0.14A^2B + 0.28A^2C \\ & + 2.31AB^2\end{aligned} \tag{5}$$

$$\begin{aligned}\text{ED} = {} & 1.41 + 0.11A \\ & + 0.013B - 9.719E{-}003C - 6.690E{-}003AB \\ & + 0.017AC + 0.028BC \\ & + 0.047A^2 - 8.429E{-}003B^2 \\ & + 0.019C^2 - 0.015ABC + 8.078E{-}003A^2B \\ & + 0.016A^2C + 0.13AB^2\end{aligned} \tag{6}$$

$$\begin{aligned}\text{EY}\ (\%) = {} & 72.53 - 5.86A - 1.63B - 2.10C - 2.21AB \\ & + 1.27AC + 2.51BC - 0.90A^2 - 0.099B^2 \\ & + 0.87C^2 - 1.23ABC + 0.92A^2B + 0.34A^2C \\ & + 7.66AB^2\end{aligned} \tag{7}$$

Table 4 Experimental design matrix with factors and their responses

Run	A (°C)	B (min)	C (°C/min)	Response 1 biochar yield (%)		Response 2 HHV (MJ/kg)		Response 3 ED		Response 4 EY (%)	
				Predicted	Exp.	Predicted	Exp.	Predicted	Exp.	Predicted	Exp.
1	500	40	4.00	46.59	46.13	28.94	29.09	1.69	1.70	78.87	78.33
2	425	47.5	5.50	51.54	51.07	24.10	24.12	1.41	1.40	72.53	71.91
3	350	40	4.00	60.79	60.32	21.24	21.39	1.24	1.25	75.87	75.32
4	500	40	7.00	43.99	43.52	29.29	29.44	1.71	1.72	75.33	74.79
5	350	55	4.00	58.58	58.11	20.73	20.88	1.21	1.22	71.38	70.84
6	425	47.5	2.98	53.53	54.20	25.27	25.06	1.48	1.46	78.52	79.29
7	425	47.5	5.50	51.54	51.16	24.10	24.05	1.41	1.40	72.53	71.83
8	425	47.5	5.5	51.54	51.94	24.10	23.92	1.40	1.39	71.53	71.89
9	425	47.5	80.23	49.84	50.50	24.71	24.50	1.44	1.43	71.45	72.22
10	425	34.89	5.5	55.49	56.16	23.32	23.11	1.35	1.34	74.99	75.76
11	350	55	7	56.80	56.33	21.83	21.98	1.27	1.28	72.83	72.28
12	425	47.5	5.5	51.54	51.60	24.10	23.92	1.40	1.39	72.53	72.05
13	551.13	47.5	5.5	34.72	35.38	29.69	29.48	1.71	1.72	60.12	60.89
14	298.87	47.5	5.5	59.72	60.38	23.08	22.87	1.35	1.34	79.84	80.61
15	425	47.5	5.5	51.54	51.94	24.10	24.36	1.41	1.42	72.53	73.86
16	350	40	7	54.50	54.03	19.44	19.59	1.13	1.14	62.34	61.79
17	425	47.5	5.5	51.54	51.74	24.10	24.29	1.41	1.42	72.53	73.36
18	425	60.11	5.5	49.83	50.50	24.05	23.84	1.40	1.39	69.51	70.28
19	500	55	4	40.59	41.13	28.98	29.13	1.69	1.70	70.48	69.93
20	500	55	7	40.82	40.35	30.21	30.36	1.76	1.77	72.06	71.51

A temperature (°C), *B* time (minutes), *C* heating rate (°C/minutes), *Exp.* experimental value

These coded equations provide an insight into the linear and interaction effects of process parameters on the selected responses. The quadratic Eq. (4) and cubic Eqs. (5, 6 and 7) regression models were found to be the most appropriate model for determining interactions between these variables. The predicted values were quite close to observed values, which infer that the model is significant. The statistical implication of polynomial models was examined by analysis of variance (ANOVA), probability (*p* value) and Fischer variation (*F* values). The fitness of model was analysed through correlation coefficient (R^2). Tables S1, S2, S3 and S4 show the variation source (linear, interaction, quadratic and cubic), coefficient, sum of squares, degree of freedom, mean sum of square, lack of fit, pure error, corrected total, along with R^2 and adj. R^2 for yield, HHV, ED and EY of biochar produced by different pyrolysis conditions. The adequacy of the model was also tested by higher *F* value of lack of fit, and lower probability (*p*) values of the parameters involved indicating model terms were significant [45, 46].

Yield of Biochar (%)

The model *F* value of 116.69 with *p* value of < 0.0001 indicated that the quadratic model were significant (Table S1). The correlation coefficient ($R^2 = 0.99$) and adjusted R^2 value (0.98) imply that most of total variations were explained by the model given in Eq. (4). The lack of fit *F* value of 13.18 corroborate that lack of fit was significant [45]. All three linear terms (*A*, *B* and *C*) considered in this study contributed significantly to the yield of biochar (*p* value lower than 0.05). Amongst the interaction effects, the interaction between temperature-time (*AB*) and time-heating rate (*BC*) was the most significant ($p < 0.05$). In addition to this, square term of the model (A^2) was also found significant (< 0.0001). On increasing the pyrolysis temperature, time and heating rate, a continuous decrease in biochar yield (%) was observed, as is evident from the response surface plots shown in Fig. 3a, b. This decrease in yield (%) of biochar at higher temperatures may be due to significant loss of volatile matter; non-condensable gases such as CO_2, H_2, CO and CH_4; dehydration of hydroxyl groups; and thermal degradation of cellulose, hemicelluloses and lignin. Similar findings were reported by Williams and Nugranad [47], wherein 7.5% decrease in biochar yield (rice husk–based biochar) was observed on increasing the temperature from 400 to 600 °C. The reduction in biochar yield when subjecting rice husk at high temperature for longer time may be due to the occurrence of thermal cracking [34]. The yield (%) of biochar was

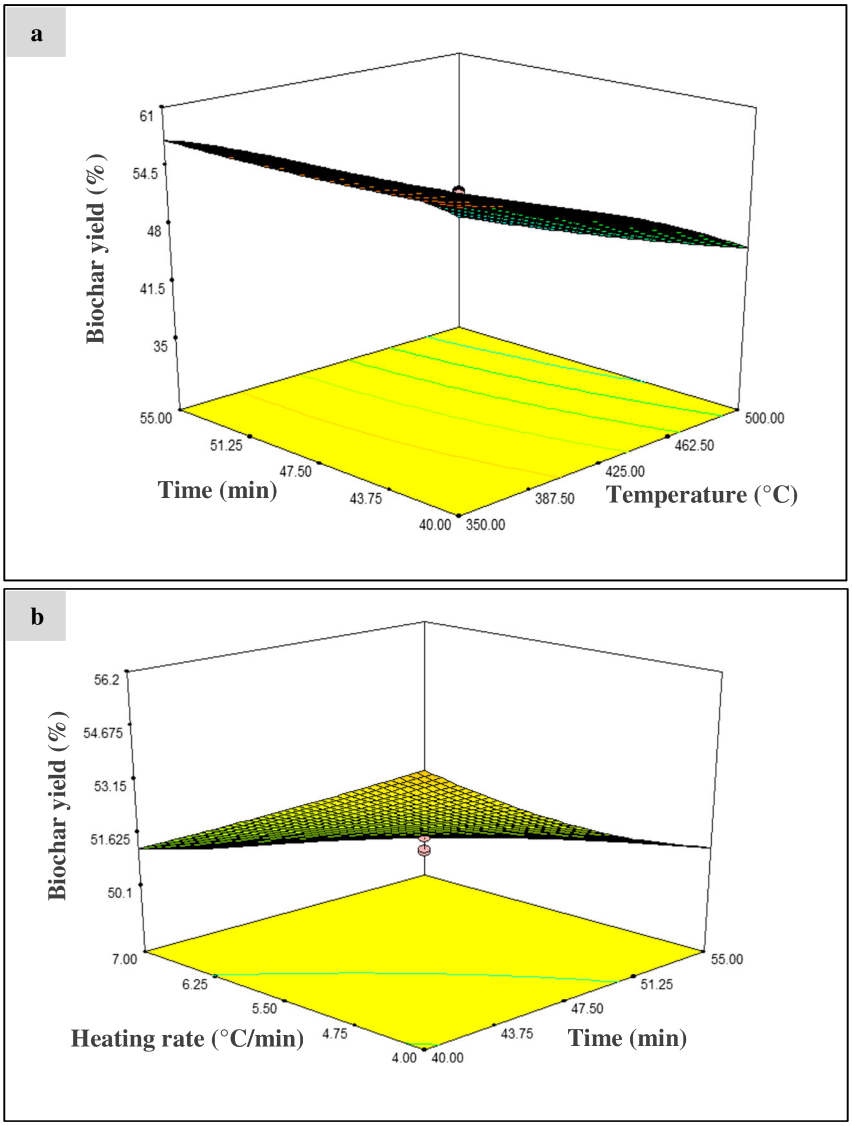

Fig. 3 Response surface plots for interactive effects of **a** time and temperature, **b** heating rate and time on percent yield of biochar

higher at low heating rate because of the absence of thermal cracking and secondary pyrolysis reactions [11]. Several other studies have also observed a decrease in biochar yield on increasing the heating rate from 30 to 50 °C/min for biomass from various feedstocks [48]. This is probably due to the fact that high heating rate was responsible for depolymerisation of biomass, leading to the formation of gaseous and volatile components and reduced biochar yield [43].

Higher Heating Value (MJ/kg)

Higher heating value (HHV) is the energy released per unit mass of biomass when it undergoes complete combustion. HHV depends upon the percentage of carbon, hydrogen, nitrogen and ash content. Higher heating value signifies synthesis of feedstock for production of an alternate and clean energy source. HHV for rice husk biomass was observed to be 17.13 MJ/kg. However, it was observed that the biochar produced at highest pyrolysis temperature of 551.13 °C yielded the maximum HHV value of 29.48 MJ/kg (run 13 in Table 4). The analysis of variance for HHV for rice husk–derived biochar with a model F value of 134.08, lack of fit F value of 13.50 and p value of < 0.0001 indicated that the model is significant (Table S2) [46]. Temperature was the most significant linear term ($p = < 0.0001$) for determination of HHV. The correlation coefficient ($R^2 = 0.99$) and adjusted R^2 value (0.98) imply that most of total variations were explained by the model given in Eq. (5). The interactions between temperature and heating rate (AC) and heating rate and time (BC) were significant with p value less than 0.05 (Fig. 4a, b). These results are in agreement with previous study [49] which reported that a high degree of carbonization was responsible for increase in HHV at

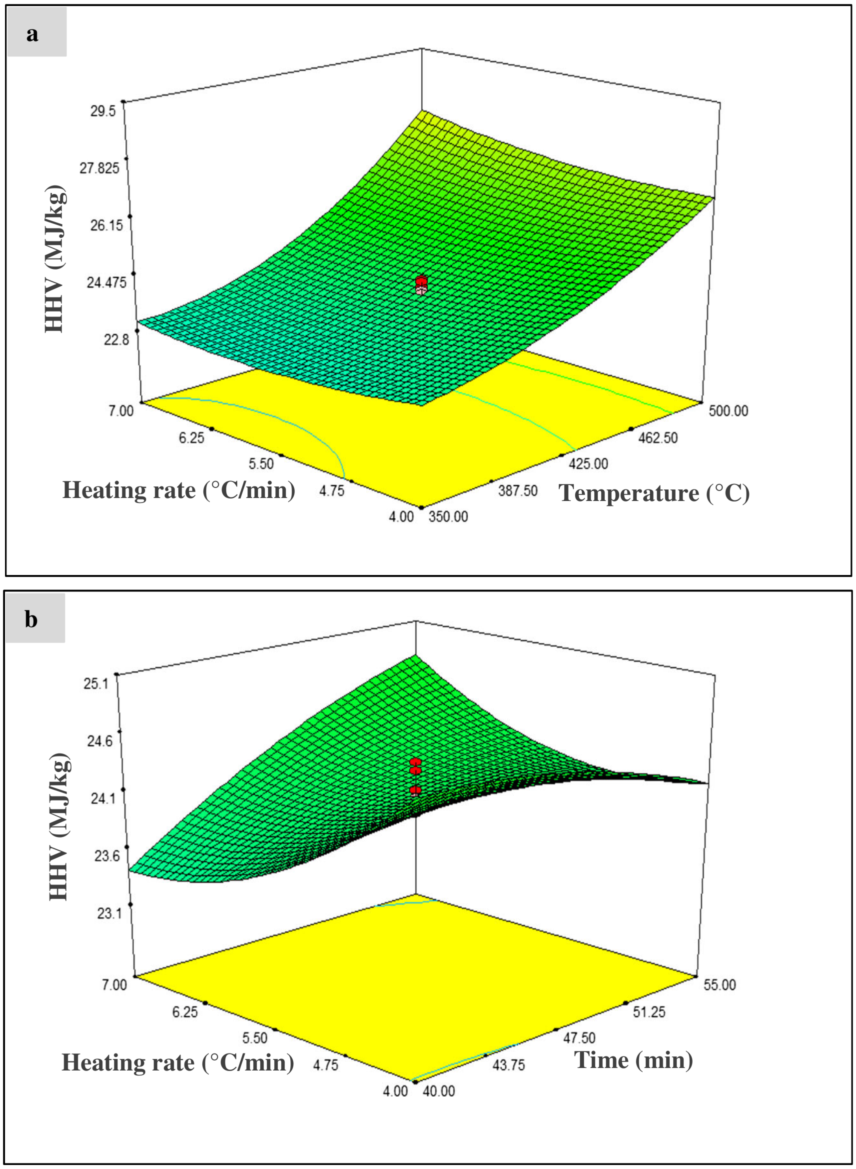

Fig. 4 Response surface plots for interactive effects of **a** heating rate and temperature, **b** heating rate and time on HHV of biochar

increased temperature due to retention of highly dense energy content of biochar. No significant effect of pyrolysis time and heating rate were found on the higher heating value [49]. Based on the HHV, rice husk biochar could find application as a potential alternative to solid fuel material and liming material for acidic soil due to increased pH of biochar produced at high temperature as shown in Table 2 and Table 4. The square and cubic terms of the model (A^2, B^2 and AB^2) were also found to be significant as suggested by their p values (< 0.0001, 0.01 and < 0.0001).

Energy Density

Temperature emerged as the most critical factor for determining the energy density of rice husk–derived biochar (Table S3). Difference between the value of correlation coefficient ($R^2 = 0.99$) and adj. R^2 (0.98) was only 0.0074, which reflects the amount of the variation that could not be explained by this model. The model F value of 134.08, lack of fit F value of 13.47 and p value of < 0.0001 indicate that the model is significant (Table S3). As observed from Table S3, two of the interaction effects, viz. temperature-heating rate and time-heating rate (AC and BC) played a significant role in energy density of biochar (Fig. 5a, b). Interactive effect of time and heating rate towards energy density was found more significant ($p = 0.0062$) than temperature-heating rate ($p = 0.0472$). This may be because energy density of biochar increased with increase in temperature and heating rate simultaneously, suggesting that biochar produced at higher temperature was highly rich in energy content per unit of volume as compared to

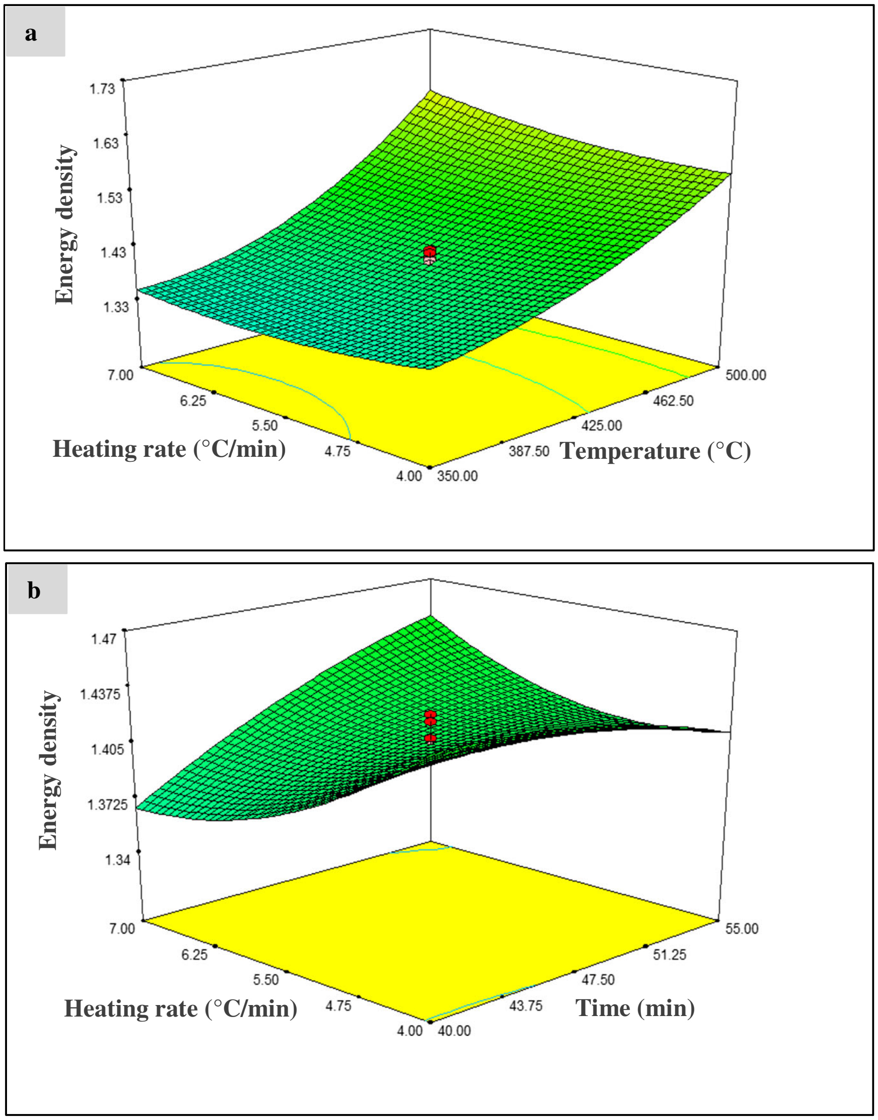

Fig. 5 Response surface plots for interactive effects of **a** heating rate and temperature, **b** heating rate and time on energy density of biochar

raw biomass. This might be due to the high degree of carbonization of organic matter present in the raw biomass [38]. The square ($A^2 = < 0.0001$, $C^2 = 0.01$) and cubic terms of the model ($AB^2 = < 0.0001$) were also found to be significant ($p < 0.0001$, $p = 0.0100$ and $p < 0.0001$).

Energy Yield (%)

The model terms A, B, C, AB, AC, BC, A^2, C^2, ABC and AB^2 were found significant ($p < 0.05$) while B^2, A^2B and A^2C were not found to be significant ($p > 0.05$) (Fig. 6a-c). Furthermore, the model F value of 19.96, lack of fit F value of 7.54 and p value of < 0.0007 with correlation coefficient ($R^2 = 0.97$) and adj. R^2 (0.92) indicated that the model is significant (Table S4). Energy yield (%) is invariably dependent on biochar yield (%) and higher heating value. Therefore, any change in biochar yield (%) and higher heating value leads to a concurrent change in its energy yield pattern. Unlike other responses, the energy yield (%) was observed to be negatively correlated with linear parameters (temperature, time and heating rate) and hence resulted in continual decrease in percent energy yield with increase of the aforementioned parameters due to the occurrence of thermal cracking at elevated pyrolysis conditions [34, 50].

Optimization

During the process of optimization, pyrolytic parameters were set to a "minimum" in order to make the thermochemical process feasible and more economical. All responses namely, biochar yield, higher heating value, energy density and energy yield were set to "maximise" because higher the values of these responses more will be the substrate available for energy. Under these conditions, the optimized values of temperature,

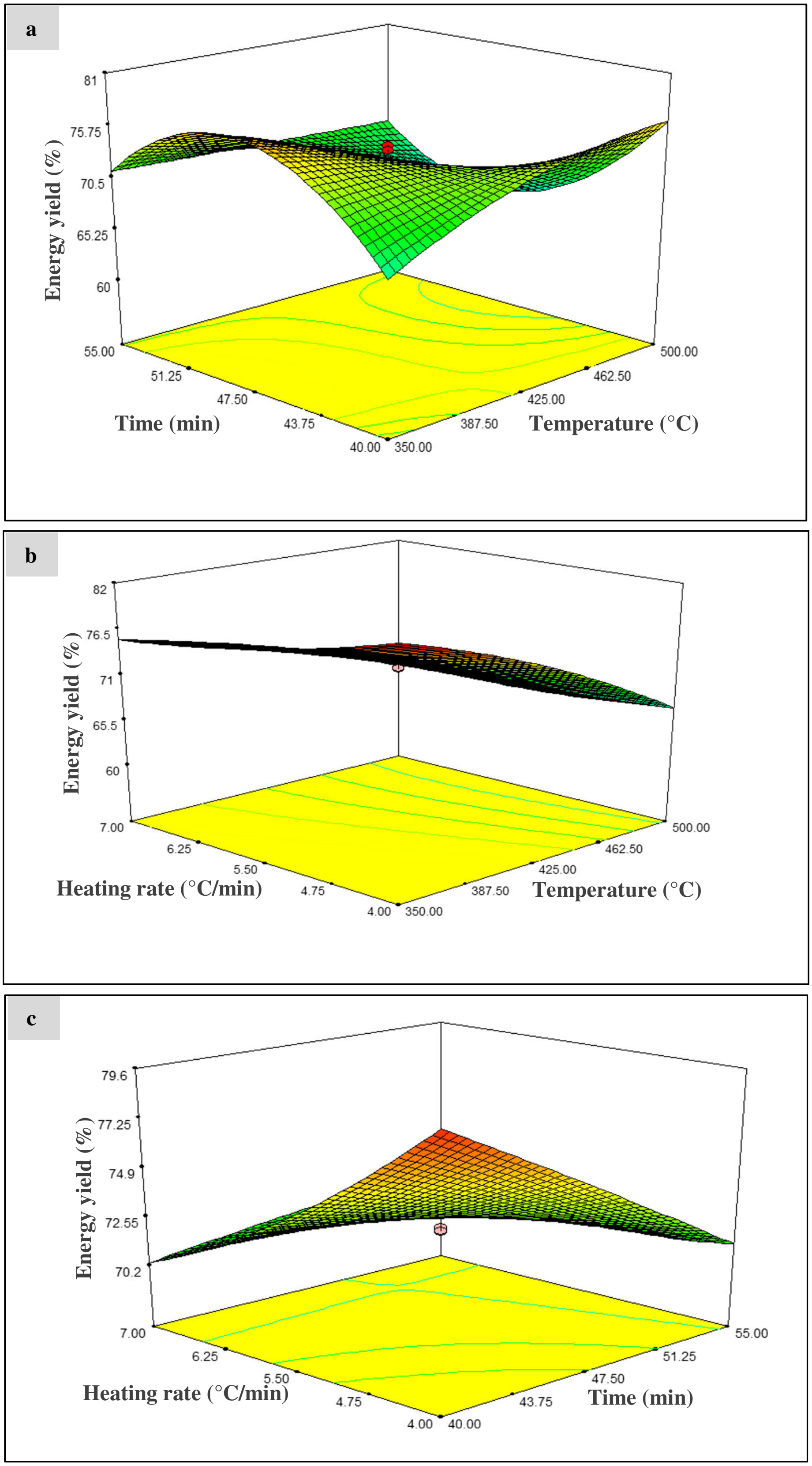

Fig. 6 Response surface plots for interactive effects of **a** time and temperature, **b** heating rate and temperature, **c** heating rate and time on energy yield of biochar

time and heating rate were 432 °C, 40 min and 4 °C/min respectively. At these optimised conditions, the predicted values for biochar yield, higher heating value, energy density and energy yield of biochar were 54.65%, 25.08 MJ/kg, 1.46 and 79.66%. Experiments were conducted to validate the predicted results and the biochar yield, higher heating value, energy density and energy yield of the optimized biochar were found to be 54.35%, 24.66 MJ/kg, 1.44 and 78.25% respectively, which were quite close to the predicted values.

Conclusion

This study is primarily dealt with the role played by process parameters (temperature, time and heating rate) on the yield and quality (higher heating value, energy density and energy yield) of biochar synthesized from rice husk. Among the process parameters tested, temperature has significant effect on the yield and quality of biochar. On subjecting to interaction effects, temperature and time followed by temperature and heating rate, time and heating rate had maximum influence on the yield and quality of produced biochar.

Furthermore, the fuel ratio of optimized biochar was found to be 2.10 which is near to that of bituminous coal having fuel ratio in range of 1.5 to 2.0. Thus, the thermal conversion of biomass can be a potential route to provide an economically viable, clean and environment friendly source of good quality solid fuel through utilization of biomass or biomass-derived waste.

Acknowledgements The authors thank DST-FIST for the support to the Department of Environmental Science and Engineering, Indian Institute of Technology (Indian School of Mines) Dhanbad.

Funding Information This research was supported by FRS Scheme of IIT(ISM) (Ref No. FRS/86/2014-2015/ESE) and PhD studentship for K.Y.

References

1. Bhattacharyya SC, Asia S (2014) Viability of off-grid electricity supply using rice husk : a case study from South Asia. Biomass Bioenergy 8:44–54. https://doi.org/10.1016/j.biombioe.2014.06.002
2. Zhao N, Li B-X (2016) The effect of sodium chloride on the pyrolysis of rice husk. Appl Energy 178:346–352. https://doi.org/10.1016/j.apenergy.2016.06.082
3. Kan T, Strezov V, Evans TJ (2016) Lignocellulosic biomass pyrolysis: a review of product properties and effects of pyrolysis parameters. Renew Sust Energ Rev 57:1126–1140. https://doi.org/10.1016/j.rser.2015.12.185
4. Yadav K, Jagadevan S (2019) Influence of process parameters on synthesis of biochar by pyrolysis of biomass: an alternative source of energy. In: Pyrolysis. IntechOpen, pp 1–14. https://doi.org/10.5772/intechopen.88204
5. Demirbas A, Caglar A, Akdeniz F, Gullu D (2010) Conversion of olive husk to liquid fuel by pyrolysis and catalytic liquefaction. Energy Sources 22:631–639. https://doi.org/10.1080/00908310050045582
6. Rajapaksha AU, Chen SS, Tsang DCW, Zhang M, Vithanage M, Mandal S, Gao B, Bolan NS, Ok YS (2016) Engineered /designer biochar for contaminant removal /immobilization from soil and water: potential and implication of biochar modification. Chemosphere 148:276–291. https://doi.org/10.1016/j.chemosphere.2016.01.043
7. Oliveira FR, Patel AK, Kumar S et al (2017) Environmental application of biochar : current status and perspectives. Bioresour Technol 246:110–122. https://doi.org/10.1016/j.biortech.2017.08.122
8. Zhang K, Cheng X, Dang H, Ye C, Zhang Y, Zhang Q (2013) Linking litter production, quality and decomposition to vegetation succession following agricultural abandonment. Soil Biol Biochem 57:803–813. https://doi.org/10.1016/j.soilbio.2012.08.005
9. Anupam K, Sharma AK, Lal PS, Dutta S, Maity S (2016) Preparation, characterization and optimization for upgrading Leucaena leucocephala bark to biochar fuel with high energy yielding. Energy 106:743–756. https://doi.org/10.1016/j.energy.2016.03.100
10. Wang T, Zhai Y, Zhu Y, Li C, Zeng G (2018) A review of the hydrothermal carbonization of biomass waste for hydrochar formation: process conditions, fundamentals, and physicochemical properties. Renew Sust Energ Rev 90:223–247. https://doi.org/10.1016/j.rser.2018.03.071
11. Tripathi M, Sahu JN, Ganesan P (2016) Effect of process parameters on production of biochar from biomass waste through pyrolysis: a review. Renew Sust Energ Rev 55:467–481. https://doi.org/10.1016/j.rser.2015.10.122
12. Ahmad M, Rajapaksha AU, Lim JE, Zhang M, Bolan N, Mohan D, Vithanage M, Lee SS, Ok YS (2014) Biochar as a sorbent for contaminant management in soil and water: a review. Chemosphere 99:19–23. https://doi.org/10.1016/j.chemosphere.2013.10.071
13. Liu Z, Quek A, Kent Hoekman S, Balasubramanian R (2013) Production of solid biochar fuel from waste biomass by hydrothermal carbonization. Fuel 103:943–949. https://doi.org/10.1016/j.fuel.2012.07.069
14. Kung CC, Zhang N (2015) Renewable energy from pyrolysis using crops and agricultural residuals: an economic and environmental evaluation. Energy 90:1532–1544. https://doi.org/10.1016/j.energy.2015.06.114
15. Jeguirim M, Bikai J, Elmay Y, Limousy L, Njeugna E (2014) Thermal characterization and pyrolysis kinetics of tropical biomass feedstocks for energy recovery. Energy Sustain Dev 23:188–193. https://doi.org/10.1016/j.esd.2014.09.009
16. Mašek O, Brownsort P, Cross A, Sohi S (2013) Influence of production conditions on the yield and environmental stability of biochar. Fuel 103:151–155. https://doi.org/10.1016/j.fuel.2011.08.044
17. Gil MV, Riaza J, Álvarez L, Pevida C, Rubiera F (2015) Biomass devolatilization at high temperature under N_2 and CO_2: char morphology and reactivity. Energy 91:655–662. https://doi.org/10.1016/j.energy.2015.08.074
18. Lin L, Yan R, Liu Y, Jiang W (2010) In-depth investigation of enzymatic hydrolysis of biomass wastes based on three major components: cellulose, hemicellulose and lignin. Bioresour Technol 101:8217–8223. https://doi.org/10.1016/j.biortech.2010.05.084
19. Yavari S, Malakahmad A, Sapari NB, Yavari S (2017) Sorption properties optimization of agricultural wastes-derived biochars using response surface methodology. Process Saf Environ Prot 109:509–519. https://doi.org/10.1016/j.psep.2017.05.002

20. Zhang C, Yang L, Rong F, Fu D, Gu Z (2012) Boron-doped diamond anodic oxidation of ethidium bromide: process optimization by response surface methodology. Electrochim Acta 64:100–109. https://doi.org/10.1016/j.electacta.2011.12.122
21. Zhao B, Connor DO, Zhang J et al (2018) Effect of pyrolysis temperature, heating rate, and residence time on rapeseed stem derived biochar. J Clean Prod 174:977–987
22. Onay O (2007) Influence of pyrolysis temperature and heating rate on the production of bio-oil and char from safflower seed by pyrolysis, using a well-swept fixed-bed reactor. Fuel Process Technol 88: 523–531. https://doi.org/10.1016/j.fuproc.2007.01.001
23. Isa KM, Daud S, Hamidin N, Ismail K, Saad SA, Kasim FH (2011) Thermogravimetric analysis and the optimisation of bio-oil yield from fixed-bed pyrolysis of rice husk using response surface methodology (RSM). Ind Crop Prod 33:481–487. https://doi.org/10.1016/j.indcrop.2010.10.024
24. Yavari S, Malakahmad A, Sapari NB, Yavari S (2017) Synthesis optimization of oil palm empty fruit bunch and rice husk biochars for removal of imazapic and imazapyr herbicides. J Environ Manag 193:201–210. https://doi.org/10.1016/j.jenvman.2017.02.035
25. Bezerra MA, Santelli RE, Oliveira EP, Villar LS, Escaleira LA (2008) Response surface methodology (RSM) as a tool for optimization in analytical chemistry. Talanta 76:965–977. https://doi.org/10.1016/j.talanta.2008.05.019
26. Tyagi M, Rana A, Kumari S, Jagadevan S (2018) Adsorptive removal of cyanide from coke oven wastewater onto zero-valent iron: optimization through response surface methodology, isotherm and kinetic studies. J Clean Prod 178:398–407. https://doi.org/10.1016/j.jclepro.2018.01.016
27. Mondal P, Mehta D, George S (2016) Defluoridation studies with synthesized magnesium-incorporated hydroxyapatite and parameter optimization using response surface methodology. Desalin Water Treat 57:27294–27313. https://doi.org/10.1080/19443994.2016.1167628
28. Wang Y, Qiu L, Zhang T, Yang X, Kang K (2019) Optimization of carbonization process for the production of solid biofuel from corn stalk using response surface methodology. Bioenerg Res 12:184–196. https://doi.org/10.1007/s12155-018-9955-7
29. Mesroghli S, Jorjani E, Chehreh Chelgani S (2009) Estimation of gross calorific value based on coal analysis using regression and artificial neural networks. Int J Coal Geol 79:49–54. https://doi.org/10.1016/j.coal.2009.04.002
30. Waqas M, Aburiazaiza AS, Miandad R, Rehan M, Barakat MA, Nizami AS (2018) Development of biochar as fuel and catalyst in energy recovery technologies. J Clean Prod 188:477–488. https://doi.org/10.1016/j.jclepro.2018.04.017
31. Ahmad M, Lee SS, Dou X, Mohan D, Sung JK, Yang JE, Ok YS (2012) Effects of pyrolysis temperature on soybean stover- and peanut shell-derived biochar properties and TCE adsorption in water. Bioresour Technol 118:536–544. https://doi.org/10.1016/j.biortech.2012.05.042
32. Devi P, Saroha AK (2015) Effect of pyrolysis temperature on polycyclic aromatic hydrocarbons toxicity and sorption behaviour of biochars prepared by pyrolysis of paper mill effluent treatment plant sludge. Bioresour Technol 192:312–320. https://doi.org/10.1016/j.biortech.2015.05.084
33. Zhang J, Liu J, Liu R (2015) Effects of pyrolysis temperature and heating time on biochar obtained from the pyrolysis of straw and lignosulfonate. Bioresour Technol 176:288–291. https://doi.org/10.1016/j.biortech.2014.11.011
34. Intani K, Latif S, Kabir AKMR, Müller J (2016) Effect of self-purging pyrolysis on yield of biochar from maize cobs, husks and leaves. Bioresour Technol 218:541–551. https://doi.org/10.1016/j.biortech.2016.06.114
35. Yuan JH, Xu RK, Zhang H (2011) The forms of alkalis in the biochar produced from crop residues at different temperatures. Bioresour Technol 102:3488–3497. https://doi.org/10.1016/j.biortech.2010.11.018
36. Kurose R, Ikeda M, Makino H, Kimoto M, Miyazaki T (2004) Pulverized coal combustion characteristics of high-fuel-ratio coals. Fuel 83:1777–1785. https://doi.org/10.1016/j.fuel.2004.02.021
37. Budai A, Wang L, Gronli M, Strand LT, Antal MJ Jr, Abiven S, Dieguez-Alonso A, Anca-Couce A, Rasse DP (2014) Surface properties and chemical composition of corncob and miscanthus biochars: effects of production temperature and method. J Agric Food Chem 62:3791–3799. https://doi.org/10.1021/jf501139f
38. Chen B, Zhou D (2008) Transitional adsorption and partition of nonpolar and polar aromatic contaminants by biochars of pine needles with different pyrolytic temperatures. Environ Sci Technol 42:5137–5143
39. Li L, Quinlivan PA, Knappe DRU (2002) Effects of activated carbon surface chemistry and pore structure on the adsorption of organic contaminants from aqueous solution. Carbon 40:2085–2100. https://doi.org/10.1016/S0008-6223(02)00069-6
40. Kumar S, Masto RE, Ram LC, Sarkar P, George J, Selvi VA (2013) Biochar preparation from Parthenium hysterophorus and its potential use in soil application. Ecol Eng 55:67–72. https://doi.org/10.1016/j.ecoleng.2013.02.011
41. Sharma RK, Wooten JB, Baliga VL, Lin X, Geoffrey Chan W, Hajaligol MR (2004) Characterization of chars from pyrolysis of lignin. Fuel 83:1469–1482. https://doi.org/10.1016/j.fuel.2003.11.015
42. Uchimiya M, Wartelle LH, Klasson KT, Fortier CA, Lima IM (2011) Influence of pyrolysis temperature on biochar property and function as a heavy metal sorbent in soil. J Agric Food Chem 59: 2501–2510
43. Ayllón M, Aznar M, Sánchez JL et al (2006) Influence of temperature and heating rate on the fixed bed pyrolysis of meat and bone meal. Chem Eng J 121:85–96. https://doi.org/10.1016/j.cej.2006.04.013
44. Cetin E, Moghtaderi B, Gupta R, Wall TF (2004) Influence of pyrolysis conditions on the structure and gasification reactivity of biomass chars. Fuel 83:2139–2150. https://doi.org/10.1016/j.fuel.2004.05.008
45. Kadlimatti HM, Mohan BR, Saidutta MB (2019) Bio-oil from microwave assisted pyrolysis of food waste-optimization using response surface methodology. Biomass Bioenergy 123:25–33. https://doi.org/10.1016/j.biombioe.2019.01.014
46. Saikia R, Baruah B, Kalita D, Pant KK, Gogoi N, Kataki R (2018) Pyrolysis and kinetic analyses of a perennial grass (Saccharum ravannae L.) from north-east India: optimization through response surface methodology and product characterization. Bioresour Technol 253:304–314. https://doi.org/10.1016/j.biortech.2018.01.054
47. Williams PT, Nugranad N (2000) Comparison of products from the pyrolysis and catalytic pyrolysis of rice husks. Energy 25:493–513. https://doi.org/10.1016/S0360-5442(00)00009-8
48. Aysu T, Küçük MM (2014) Biomass pyrolysis in a fixed-bed reactor: effects of pyrolysis parameters on product yields and characterization of products. Energy 64:1002–1025. https://doi.org/10.1016/j.energy.2013.11.053
49. Hmid A, Mondelli D, Fiore S, Fanizzi FP, al Chami Z, Dumontet S (2014) Production and characterization of biochar from three-phase olive mill waste through slow pyrolysis. Biomass Bioenergy 71: 330–339. https://doi.org/10.1016/j.biombioe.2014.09.024
50. Huang YF, Cheng PH, Te Chiueh P, Lo SL (2017) Leucaena biochar produced by microwave torrefaction: fuel properties and energy efficiency. Appl Energy 204:1018–1025. https://doi.org/10.1016/j.apenergy.2017.03.007